

論文 / 著書情報  
Article / Book Information

Title	Digital color management in full-color holographic three-dimensional printer
Authors	Fei Yang, Yuri Murakami, Masahiro Yamaguchi
Citation	Applied Optics, Vol. 51, No. 19, pp. 4343-4352
Pub. date	2012, 6
Copyright	Copyright (c) 2012 Optical Society of America
Note	<p>This paper was published in Applied optics and is made available as an electronic reprint with the permission of OSA. The paper can be found at the following URL on the OSA website: <a href="http://www.opticsinfobase.org/ao/abstract.cfm?uri=ao-51-19-4343">http://www.opticsinfobase.org/ao/abstract.cfm?uri=ao-51-19-4343</a> . Systematic or multiple reproduction or distribution to multiple locations via electronic or other means is prohibited and is subject to penalties under law.</p>

# Digital color management in full-color holographic three-dimensional printer

Fei Yang,<sup>1,\*</sup> Yuri Murakami,<sup>2</sup> and Masahiro Yamaguchi<sup>2</sup>

<sup>1</sup>Interdisciplinary Graduate School of Science and Engineering, Tokyo Institute of Technology, 4259-S1-17 Nagatsuta, Midori-ku, Yokohama, Kanagawa 226–8503, Japan

<sup>2</sup>Global Scientific Information and Computing Center, Tokyo Institute of Technology, 2-12-1-I7-6 Meguro-ku, Tokyo 152–8550, Japan

\*Corresponding author: yang.f.aa@m.titech.ac.jp

Received 8 March 2012; revised 5 May 2012; accepted 16 May 2012;  
posted 17 May 2012 (Doc. ID 164397); published 25 June 2012

We propose a new method of color management for a full-color holographic, three-dimensional (3D) printer, which produces a volume reflection holographic stereogram using red, green, and blue three-color lasers. For natural color management in the holographic 3D printer, we characterize its color reproduction characteristics based on the spectral measurement of reproduced light. Then the color conversion formula, which comprises a one-dimensional lookup table and a  $3 \times 3$  matrix, was derived from the measurement data. The color reproducibility was evaluated by printing a color chart hologram, and the average CIELAB  $\Delta E = 13.19$  is fairly small. © 2012 Optical Society of America  
OCIS codes: 000.2170, 090.1705.

## 1. Introduction

A holographic three-dimensional (3D) printer (holo-printer), which automatically produces a holographic stereogram (HS) from the 3D image data generated or processed in a computer, has been developed [1–7]. In particular, the system for recording full-parallax HS as a volume reflection hologram [1] enables output of high-quality and full-color 3D displays by using three lasers with red, green, and blue (RGB) colors [8,9]. The reproduction of a color is one of the important factors in full-color holographic displays, and excellent results on the color reproduction in volume reflection holograms have been reported [10]. However different approach is needed in the system for printing HS from digital 3D data. This article presents a system that incorporates digital color management in a full-color, full-parallax holoprinter and shows the result of evaluating its color reproducibility.

In digital media for color image reproduction, such as color displays and printers, a digital color

management technique has been introduced. The characterization of a display device is a basic process in color management, which aims to reproduce the color from the digital count defined on given tristimulus values. The characterization of display devices as cathode-ray tubes (CRTs) and liquid crystal displays (LCDs) has been extensively studied, and the standard format for the profile data, called the International Color Consortium (ICC) profile, has been widely used. It is often possible to assume that the color is spatially uniform and the color coordinates of primary colors are constant, and each color channel is independent of the levels of other color channels in the characterization of displays [11]. Then a classical model of color display [12], in which a  $3 \times 3$  matrix and one-dimensional (1D) lookup table (LUT) for color conversion, can be employed. But no report on the color reproducibility of HS has been reported until now.

For the color recording of HS as a volume reflection hologram, two schemes have been tried: multiple exposure [8] and primary color mosaic [9]. In [7], the characterization of reproduced color was investigated for the multiple-exposure hologram, and it was

shown that the cross talk between the RGB channels is significant. In this article, we adopt the recording scheme of RGB mosaic arrangement to avoid the cross talk, which is quite difficult to be calibrated. The color reproduction was characterized by recording small holograms of color patches, and the reproduced colors were measured using the optical system for diffraction efficiency measurement. In order to evaluate the color reproducibility of full-parallax HS, we recorded a color chart hologram of the GretagMacbeth ColorChecker. As a result, it was shown that the classical model works well for the color HS in which the color pixels were recorded as an RGB mosaic arrangement. It should be also considered that the color reproduced by a volume hologram depends upon the illumination geometry. The color shift due to the different illumination angle was also evaluated in the experiment.

## 2. Optical System for Full-color Holographic 3D Printer

### A. Recording System

In full-color holoprinter [8,9], we use the three laser wavelengths of red: 633 nm (He-Ne); green: 532 nm (diode-pumped solid-state, shortly DPSS); and blue: 473 nm (DPSS). The schematic recording system is shown in Fig. 1. The laser beam to be used for recording is switched by the acousto-optic modulator

(AOM) shutter placed in front of each laser. To adjust the intensity ratio of reference beams and object beams for each RGB color, we use a  $\lambda/2$  plate and a polarization beam splitter for dividing the light. The laser beam of each color passes another  $\lambda/2$  plate, which enables adjustment of the polarization of the reference and object beams. After being divided by the beam splitter, the laser beams of the three colors are combined into a single beam. The gathered laser beams, both the reference beam and the object beam, are focused into a mask size in the position of the recording medium. The reference beam is set to an angle of 30 deg from the optical axis. As the recording medium, we use a silver halide recording material (PFG-03 C, UAB Geola) [13].

In synthesizing a two-dimensional (2D) array of elementary holograms, the recording medium is set on an X-Y stage, and after the exposure of an elementary hologram it moves to the following exposure portion. The size of each elementary hologram is  $200\ \mu\text{m} \times 200\ \mu\text{m}$  in the experiment, where each elementary hologram holds a 2D image. To control the size of the elementary hologram, the apertures are set between the LCD and the hologram plate for the object beam, and between the mirror  $M_{10}$  and the lens  $L_4$  for the reference beam. In the case of recording the planar color patch, a uniform image is displayed on the LCD.

There are two ways to record color holograms: space division exposure (primary color mosaic)

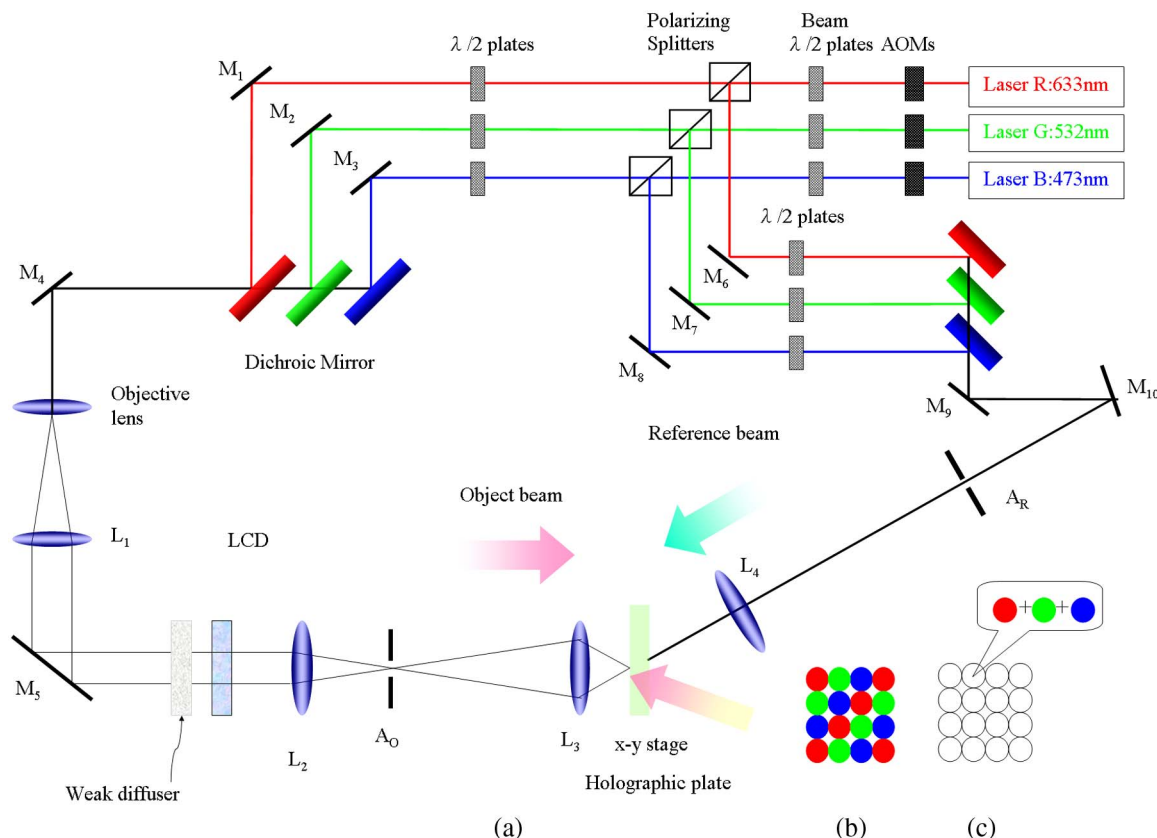


Fig. 1. (Color online) Setup of the optical recording system and the mosaic scheme for color hologram. (a) Recording system:  $L_1 - L_4$ ,  $M_1 - M_{10}$ , and  $A_0$  and  $A_R$  represent lenses, mirrors, and apertures, respectively. (b) Space-division exposure (primary color mosaic). (c) Multi-exposure.

[Fig. 1(b)] and multi-exposure, or simultaneous exposure at each elementary hologram [Fig. 1(c)]. In multiple or simultaneous exposure, the cross talk between the color channels makes it difficult to characterize the color reproduction model [8]. In this article, therefore, we consider only the color holograms of space division exposure to avoid the cross talk. Note that in the case of space division exposure, the diffracted light intensity will be decreased to one-third of that of monochromatic exposure because of its recording density. On the other hand, the light intensity diffracted by multi-exposure depends on the dynamic range of the recording material because three different gratings are recorded in the same region of the hologram.

In order to record each elementary hologram, the whole LCD was illuminated by the laser beam of the corresponding color. The image displayed on the LCD is the corresponding color channel of the projection image, which is calculated beforehand using 3D graphical rendering so that a 3D image is reconstructed by light-field reproduction. Red, green, and blue elementary holograms are sequentially recorded on different regions on the hologram plane so as not to overlap each other.

The LCD panel used in the optical system is a twisted-nematic electronically addressed liquid crystal panel of  $640 \times 480$  pixels, and image data from the computer is displayed on the LCD. The image data for exposure of each elementary hologram is calculated beforehand using 3D graphical rendering so that a 3D image is reconstructed by light-field reproduction. As noted in Fig. 1(a), there is a weak diffuser plate placed just before the LCD panel for making uniform the intensity distribution of the object light on the recording medium and producing a high-efficiency hologram.

To evaluate the HS produced by the system described above, we measured the color and diffraction efficiency of the HS by exposing planar color patches with the size of  $5 \text{ mm} \times 5 \text{ mm}$  ( $25 \times 25$  dots as  $200 \text{ } \mu\text{m} \times 200 \text{ } \mu\text{m}$  elementary holograms). In the case of recording the planar color patch, a uniform image is displayed on the LCD.

The development processing of the material is as follows:

Hardening: formalin hardener	6 min	20 °C
Flushing: water	4 min	
Development: CW-C1	5 min	20 °C
Stopping: ethylic acid	30 s	20 °C
Bleaching: EDTA	10 min	20 °C
Perform natural dryness after flush.		

## B. Measurement System

The measurement system for investigating the color and diffraction efficiency of the HS, shown in Fig. 2(a), is the optical system for measuring the integral diffraction efficiency of the diffuse-type holograms with a xenon lamp as a white light source, which was produced by Hamamatsu Photonics K.K.

The power of the lamp is 150 W, and the collimated light is used as illumination.

In Fig. 2(a), all diffracted light from the holographic media is focused on a screen (white reflectance standard), and the spectral radiance of the reconstructed image on the screen is measured by a spectroradiometer (PhotoResearch PR650). We use an aluminum mirror as the calibration sample to measure the radiance of the illumination spectrum. Then the spectral radiance of the reconstructed image on the screen is measured, and the diffraction efficiency is evaluated by the peak value of the hologram diffraction spectrum divided by the radiance of the illuminant spectrum at the same wavelength.

In general, the diffraction efficiency is measured using the illuminating beam, transmitted beam, and diffracted beam, without using a diffuser as a screen, where the hologram is a simple grating. However, in the case of the hologram here, which reconstructs diverging light rays from each elementary hologram, all the diffracted rays should be collected by the imaging lens. For the spectral measurement, the light flux within a certain solid angle is needed because of the use of a grating in the spectrometer. Thus a diffuser is used to mingle the light rays traveling in different directions into the limited solid angle. The diffraction angle from the hologram recorded by the current holoprinter system is 28.3 deg. As the angle range that can be corrected by the lens in Fig. 2(a) is approximately 32 deg, all the diffracted light from the hologram can be measured by the setup in Fig. 2(a).

On the other hand, in calculating colors, we first calculate the International Commission on Illumination (CIE) 1931 XYZ tristimulus values by

$$g_i = \int C_i(\lambda)H(\lambda)I(\lambda)d\lambda, \quad (1)$$

where  $C_i(\lambda)$  is the CIE 1931 XYZ color matching functions,  $H(\lambda)$  the spectral diffraction efficiency of the hologram,  $I(\lambda)$  the illuminant spectrum, and  $i = X, Y, Z$ , respectively.

Figure 2(b) shows another optical setup for measuring reproduced color by more realistic geometry simulating the actual observation of the reconstructed 3D image. This system is also employed to evaluate the color reproduction when the illumination angle is varied.

## 3. Model of Holographic 3D Printer Color Reproduction

The models of color reproduction in computer-controlled color displays have been studied for CRT, LCD, and other types of monitors [11,12,14]. In conventional models for CRT and LCD, some assumptions are made and evaluated so that the input and output characteristics are represented by a simple formula [15,16].

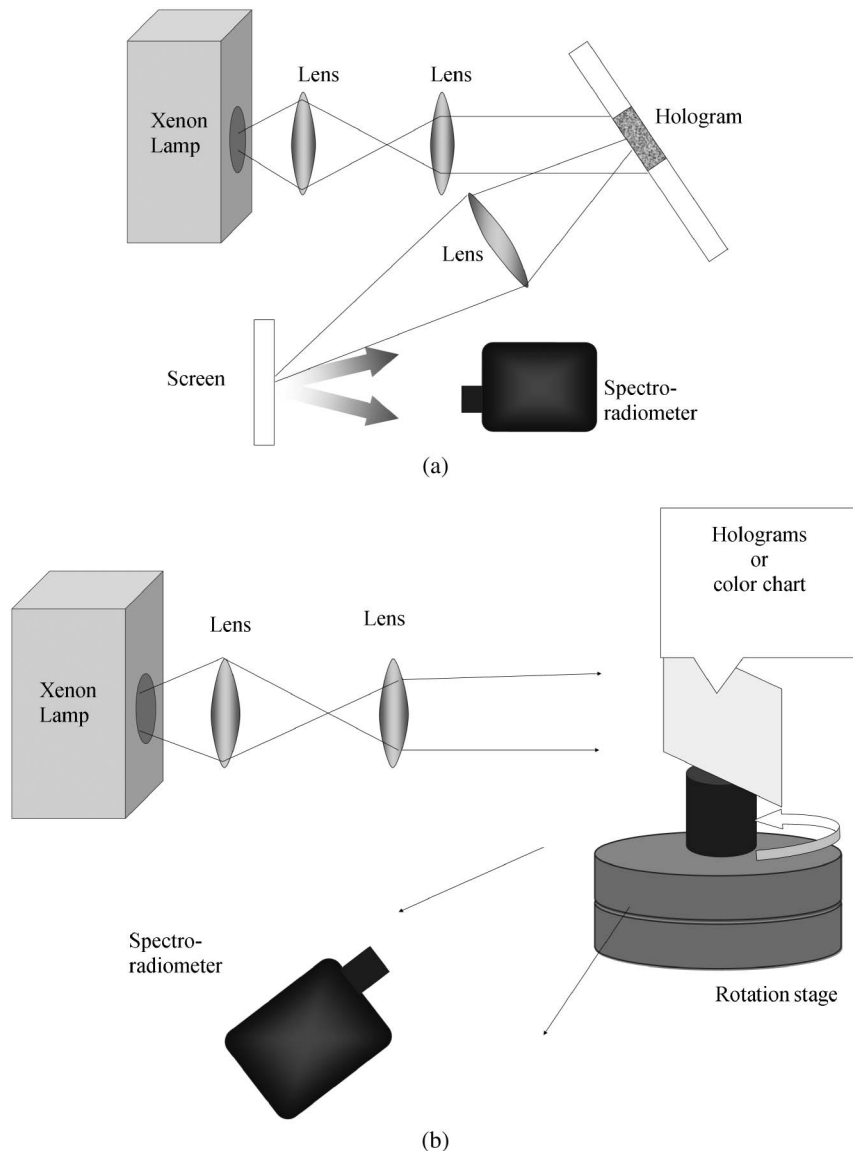


Fig. 2. Measurement optical systems. (a) Optical system for the measurement of diffraction efficiency and color of HS. (b) Optical system for measurement of the reconstructed light at changing illumination angle.

#### A. Assumption for the Forward Model

Channel constancy of a color display implies that the relative spectrum emitted by a three-color elementary hologram is independent of input gray level of the corresponding color channel (specifically, in the system of Fig. 1, it is the input gray level of the LCD that modulates the object beam). If the thickness of the recording material changes, the wavelength of the reconstructed light will shift according to the Bragg condition. The assessment of this assumption is presented in Subsection 4.D.

The color reproduction model of the holoprinter characterizes the relationship between the RGB digital counts delivered to the LCD and the tristimulus values of the reproduced image. If the channel independence assumption is satisfied, the red component of the reproduced image is determined by the input red digital count only; that is, no cross talk should be taken

into account. In the case of multiple exposure of red, green, and blue elementary holograms, it is very difficult to meet this assumption. The three mosaic, space-division-exposure components are recorded independently, and channel independence is considered to be satisfied.

Spatial homogeneity is another important assumption in color management. It may be affected by the spatial distribution of reconstruction light, the spatial homogeneity of object beam, the stability of the recording optical system, and the chemical process for development. It is not completely satisfied in the current printing system because the optical system setting is not completely fixed. However, in the preliminary investigation for color characterization, the spatial inhomogeneity may be ignored because it can be reduced by setting the system more carefully.

In 2D color displays, pixel independence is another important aspect for accurate color characterization.



In HS, we should take into account the independence of each light ray recorded in each elementary hologram. The light rays diverging from a single point on the hologram plane are recorded in an elementary hologram, and these rays are affected by each other if there is a nonlinearity in the recording material. As a result, we should consider the cross talk between the light rays. Although the cross talk should be addressed in the color characterization of HS, we disregard the issue in this article as the first step. This issue is left for future investigation.

With our measurement optical system, the collimated illumination incident angle here performs an important role for HS color reproduction. We will explain details of the experiment and the variation depending on the illumination incident angle changes in Subsection 4.E.

#### B. Forward Model

If the above assumptions hold in the HS recording and reconstruction system, we obtain the following forward model:

$$H_e(\lambda) = R'f_r(\lambda) + G'f_g(\lambda) + B'f_b(\lambda) + f_{bg}(\lambda), \quad (2)$$

where  $H_e(\lambda)$ ,  $f_r(\lambda)$ ,  $f_g(\lambda)$ ,  $f_b(\lambda)$ , and  $f_{bg}(\lambda)$  are the spectral radiance of the reconstructed light, the RGB primaries with their maximum radiance, and the background light, respectively, and  $R'$ ,  $G'$ , and  $B'$  are the coefficients for the LCD RGB channels, respectively. This model represents that the reconstructed spectrum of each primary color is the additive mixture of RGB primary spectra to reproduce the reconstructed spectrum of a hologram. From the tone reproduction characteristics of HS,  $\gamma_k\{\}$ , ( $k = r, g, b$ ),  $R'$ ,  $G'$ , and  $B'$  are expressed as follows:

$$R' = \gamma_r\{R\}, \quad G' = \gamma_g\{G\}, \quad B' = \gamma_b\{B\}, \quad (3)$$

where  $R$ ,  $G$ , and  $B$  are the input digital counts delivered to the RGB channels of the LCD, respectively.

Applying Eq. (1) to Eq. (2), we have

$$\begin{pmatrix} X \\ Y \\ Z \end{pmatrix} = \begin{pmatrix} X_r & X_g & X_b \\ Y_r & Y_g & Y_b \\ Z_r & Z_g & Z_b \end{pmatrix} \begin{pmatrix} R' \\ G' \\ B' \end{pmatrix} + \begin{pmatrix} X_{bg} \\ Y_{bg} \\ Z_{bg} \end{pmatrix}, \quad (4)$$

where

$$\begin{pmatrix} X_k \\ Y_k \\ Z_k \end{pmatrix} = \begin{pmatrix} \int C_X(\lambda)f_k(\lambda)d\lambda \\ \int C_Y(\lambda)f_k(\lambda)d\lambda \\ \int C_Z(\lambda)f_k(\lambda)d\lambda \end{pmatrix}, \quad (5)$$

and  $k = r, g, b$ , and  $bg$ .

In order to make the forward model, Eq. (6), we have to measure the XYZ values of the RGB primaries with their maximum radiance. However, the radiance changes depending on the illumination conditions such as the power and the angle of illumination lights.

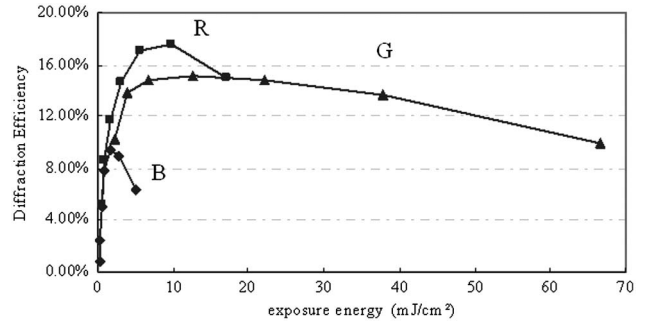


Fig. 3. Relation between the exposure amount and the diffraction efficiency for each color.

It is convenient if we define the forward model independent of the absolute radiance of the reconstructed light. We use another expression of the forward model, which includes the chromaticity coordinates of RGB primaries and the luminance of white,  $Y_w$ . The model is expressed by

$$\begin{pmatrix} X \\ Y \\ Z \end{pmatrix} = Y_w \begin{pmatrix} x_r r & x_g g & x_b b \\ y_r r & y_g g & y_b b \\ z_r r & z_g g & z_b b \end{pmatrix} \begin{pmatrix} R' \\ G' \\ B' \end{pmatrix} + \begin{pmatrix} X_{bg} \\ Y_{bg} \\ Z_{bg} \end{pmatrix} \quad \text{and} \quad (6)$$

$$\begin{pmatrix} r \\ g \\ b \end{pmatrix} = \begin{pmatrix} x_r & x_g & x_b \\ y_r & y_g & y_b \\ z_r & z_g & z_b \end{pmatrix}^{-1} \begin{pmatrix} \frac{x_w}{y_w} \\ 1 \\ \frac{z_w}{y_w} \end{pmatrix},$$

where  $(x_w, y_w, z_w)$ ,  $(x_r, y_r, z_r)$ ,  $(x_g, y_g, z_g)$ , and  $(x_b, y_b, z_b)$  are the reproduced chromaticity coordinates  $(x, y, z)$ , of gray patch and RGB primary holograms, respectively [17].

#### C. Inverse Model

The inverse model for color reproduction in HS is the conversion from the XYZ tristimulus values of the original object to the device-dependent digital count (RGB). It is derived by taking the inverse of Eqs. (3) and (6), as follows:

$$\begin{pmatrix} R' \\ G' \\ B' \end{pmatrix} = M \left\{ \begin{pmatrix} X \\ Y \\ Z \end{pmatrix} - \begin{pmatrix} X_{bg} \\ Y_{bg} \\ Z_{bg} \end{pmatrix} \right\}, \quad (7)$$

where

$$M = \begin{pmatrix} x_r r & x_g g & x_b b \\ y_r r & y_g g & y_b b \\ z_r r & z_g g & z_b b \end{pmatrix}^{-1}$$

Table 1. Exposing Condition of Lasers

Wavelength (nm)	Exposure (mJ/cm <sup>2</sup> )	$\eta$ (diffraction efficiency) (%)
R (633)	9.7	17.6
G (532)	12.5	15.1
B (473)	1.7	9.36

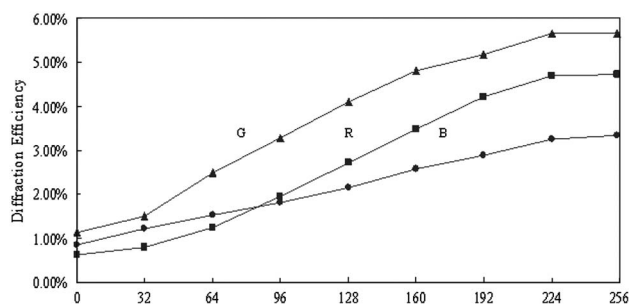


Fig. 4. Gray levels of LCD with its diffraction efficiency by space-division exposure.

and

$$R = \gamma_r^{-1}\{R'\}, G = \gamma_g^{-1}\{G'\}, B = \gamma_b^{-1}\{B'\}. \quad (8)$$

Thus, the transform can be implemented with matrix multiplication and the 1D LUT.

#### 4. Experimental System Calibration

##### A. Exposure Condition

The color reproduction characteristics of HS strongly depend on the exposure condition setting, such as the object light (S) to reference light (R) ratio and exposure time. Considering the sensitivity of the recording medium for each color in this system, we investigated the optimum exposure conditions of each color in monochrome exposure. First, we examined the S/R ratio. Through the experiment, test exposures were performed with different S/R ratios,

and it was found that the case of S/R ratio being 1:5 of the red and green lasers, and 1:2 of the blue laser, is approximately the best condition.

Next, we examined the amount of exposure of each color. We set the above S/R ratio settings and exposed in the order of red, green, and blue. A uniform image is displayed on the LCD panel, whose tone values for red, green, and blue are the maximum, namely 255, as the digital count driving the LCD has 8 bits gray scale (255 levels). We produced a HS per these conditions and measured the diffraction efficiency using the optical system shown in Fig. 2(a).

The relationship between the exposure energy, which is the sum of both object and reference beams, and the diffraction efficiency is shown in Fig. 3. The condition for acquiring the highest diffraction efficiency for each of the RGB colors in a single exposure are obtained from the plots of Fig. 3 as shown in Table 1.

##### B. Determination of Color Balance

Even though the optimal exposure condition of each color is given in Table 1, the reproduced color is not balanced. Thus we investigated space-division exposure conditions when the diffraction efficiency for each color becomes approximately equal.

Ideally, the amount of exposure can be determined from Fig. 3 as each RGB element is recorded independently in the space-division exposure. However, the diffraction efficiencies of red, green, and blue that were actually obtained did not reach the same level. This is due to the fact that the adjacent elementary holograms are slightly overlapped with each other.

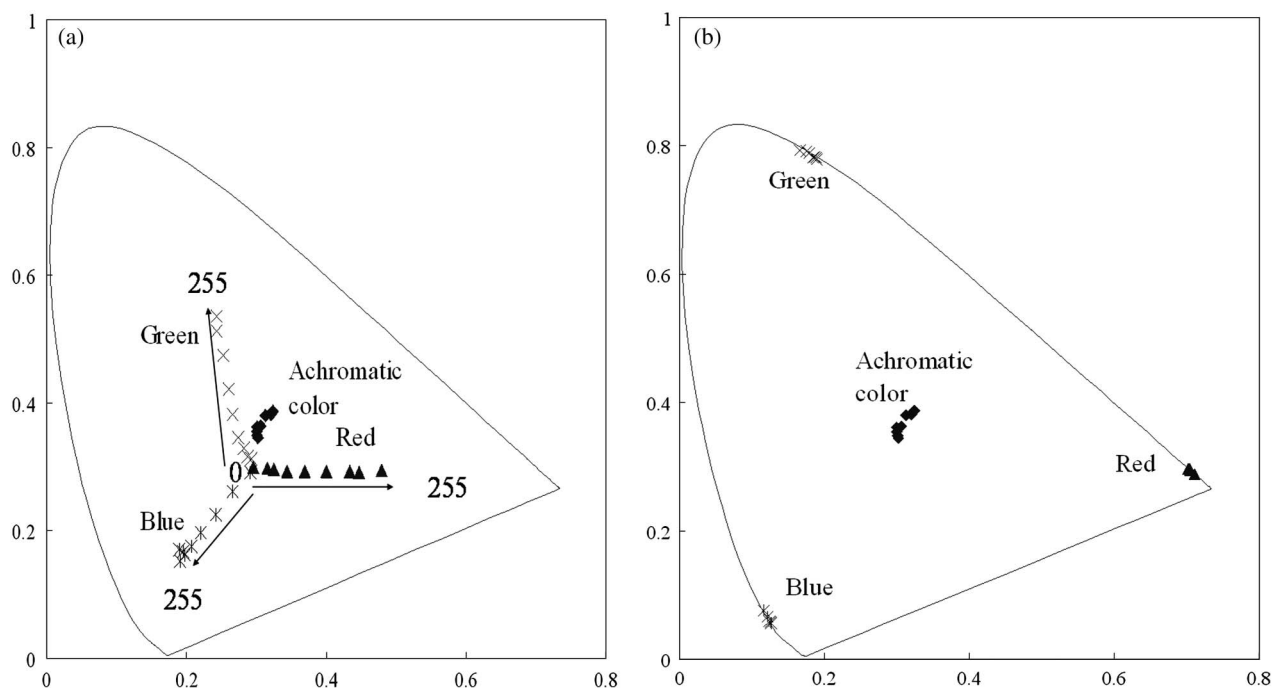


Fig. 5. Chromaticity diagram (a) before and (b) after background compensation. Triangle-, cross-, star-, and diamond-shaped markers represent the chromaticity coordinates of the reconstructed light when input gray levels of  $(R, G, B)$  are  $(d, 0, 0)$ ,  $(0, d, 0)$ ,  $(0, 0, d)$ , and  $(d, d, d)$ , where  $d = 0, 32, 64, 96, 128, 160, 192, 224$ , and 255, respectively.

**Table 2. Chromaticity Coordinates of RGB Primary Colors and White**

	Red	Green	Blue	White
$x$	0.705	0.183	0.124	0.318
$y$	0.295	0.785	0.061	0.351
$z$	0	0.032	0.815	0.330

Therefore, we changed the amount of exposure of each color slightly to find the best condition for space-division exposure of the color hologram: the energies of red, green, and blue exposures were 1.7 mJ/cm<sup>2</sup>, 2.2 mJ/cm<sup>2</sup>, and 1.7 mJ/cm<sup>2</sup>, respectively.

### C. Tone Reproduction Curve

In the first step of color characterization, we investigated the relation between the input digital count (red, green, and blue) of the LCD and the diffraction efficiency for space-division exposure.

In the experiment, color patches (5 mm × 5 mm) were recorded while changing the gray level of the LCD from 0 to 255 by steps of 32. Then, we measured each produced color patch using the optical system shown in Fig. 2(a) and investigated the diffraction efficiency of each color. The relation between each liquid-crystal gray level for red, green, and blue and their diffraction efficiency are shown in Fig. 4. The curves shown in Fig. 4 are interpolated to derive  $\gamma k\{\}$  of Eq. (3), and  $\gamma k^{-1}\{\}$  is implemented with the 1D LUT.

### D. Channel Constancy of Full-color Full-parallax 3D Holoprinter

The color of the reconstructed images from the hologram color patches obtained above are plotted on an  $x$ - $y$  chromaticity diagram [Fig. 5(a)]. The result shows that the color approaches to the achromatic

color (center of the diagram) as the input gray level becomes low. This is due to the background light ( $X_{bg}, Y_{bg}, Z_{bg}$ )<sup>t</sup>, in Eq. (2). To compensate for the background light influence, the XYZ values of the background light were obtained by measuring the hologram recorded at the LCD's gray level = 0 for all three channels. Then, the background XYZ was subtracted from the reproduced color of each hologram so as to obtain the color component modulated by red, green, and blue primaries. This result is shown in Fig. 5(b). The result indicates that the chromaticity coordinates of the reconstructed light from the single-color hologram do not change even when the input gray level changes. That is, we can say that the channel constancy assumption is approximately satisfied.

After the subtraction of background light as shown in Fig. 5(b), the three spots appearing in the red, green, and blue areas of the spectrum locus, the chromaticity coordinates of RGB primaries, are given as shown in Table 2.

### E. Deriving Color Conversion Matrix

In the color reproduction model, we assume constant channel chromaticity, channel independence, and spatial independence. Then ( $R, G, B$ ) is obtained as (0.868, 0.861, 1.117) from Eq. (6) and the data presented in Table 2, and we derived the matrix  $\mathbf{M}$  using Eq. (8):

$$\mathbf{M} = \begin{pmatrix} 1.81 & -0.41 & -0.24 \\ -0.69 & 1.64 & -0.02 \\ 0.02 & -0.05 & 1.10 \end{pmatrix}. \quad (9)$$

By using this matrix and the tone reproduction curves presented in Subsection 4.C, we can convert

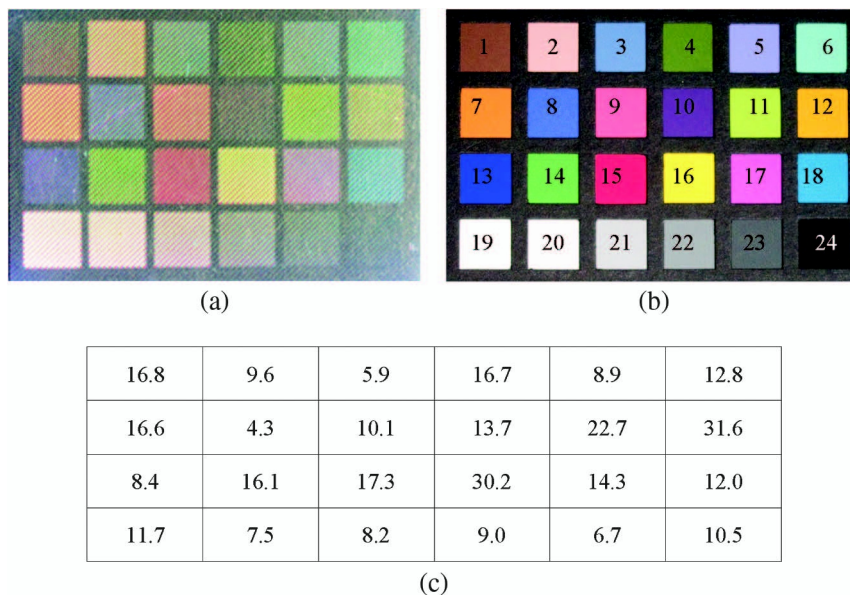


**Fig. 6. Evaluation of color chart hologram. (a) Reconstruction hologram of color chart hologram. (b) MCC color chart under xenon lamp. (c) Color difference at the incident angle of 38 deg.**



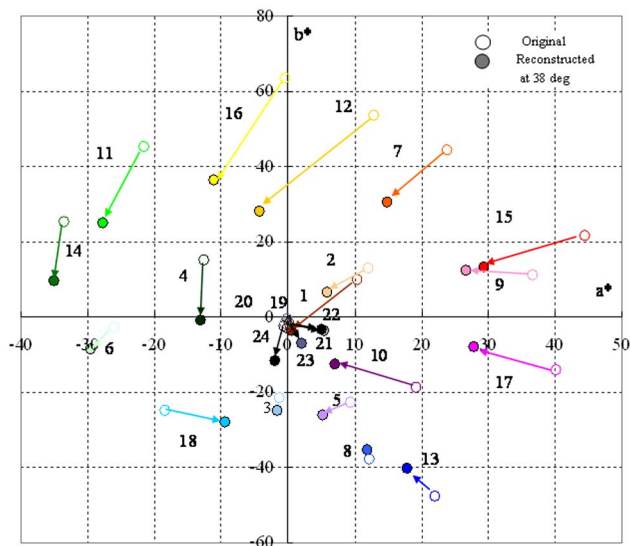


Fig. 7. (Color online) Original and reproduced colors in CIE  $a^*b^*$  plane.

XYZ tristimulus values of the original object to device-dependent digital counts ( $R$ ,  $G$ ,  $B$ ).

If the chromaticity coordinates of the three primary colors and white change, the matrix in Eq. (9) can be recalculated using Eqs. (6) and (8). When the recording medium or exposure condition changes, the peak wavelength of the reconstructed light or the color balance of the white changes. Therefore, it is reasonable to consider that the derived matrix should be recalculated for the experimental condition.

## 5. Evaluation Using Color Chart Hologram

### A. Reconstruction of Color Chart

Based on the matrix we derived, we calculated the RGB values of the color chart (GretagMacbeth ColorChecker, MCC) from its reflectance measured using a spectroradiometer under the xenon lamp illumination, and exposed the color chart hologram. In the hologram, the color chart is reconstructed on the

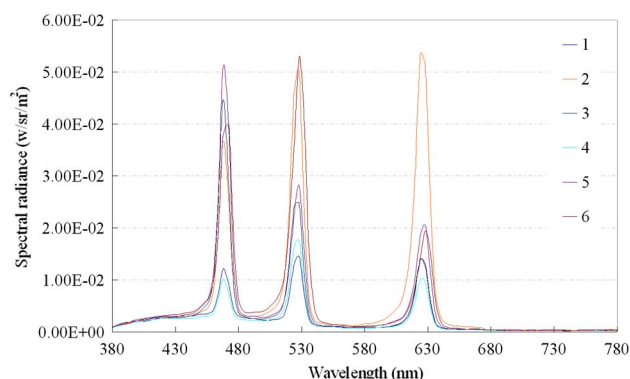


Fig. 8. (Color online) Reconstructed spectra of selected color patches in MCC where the numbers in the legend correspond to the numbers shown in Fig. 6. Incident angle of illumination light was  $32^\circ$ .

hologram plane; i.e., the images for exposure retain all uniform RGB values calculated by the above equations. Each color patch size is  $30 \times 30$  dots where the pitch of elementary holograms is  $200 \mu\text{m} \times 200 \mu\text{m}$ .

The reconstructed image of the color chart is shown in Fig. 6(a). We can see the periodic fringes on the reconstructed image; the periodic structure appearing on the reconstructed image is a color mosaic, where the size and the pitch of the elementary hologram were both  $200 \mu\text{m} \times 200 \mu\text{m}$ . By reducing the size of the elementary hologram, such artifacts will be negligible. In order to evaluate the result, we compared the colors reproduced by the hologram with a real color chart under the same xenon lamp

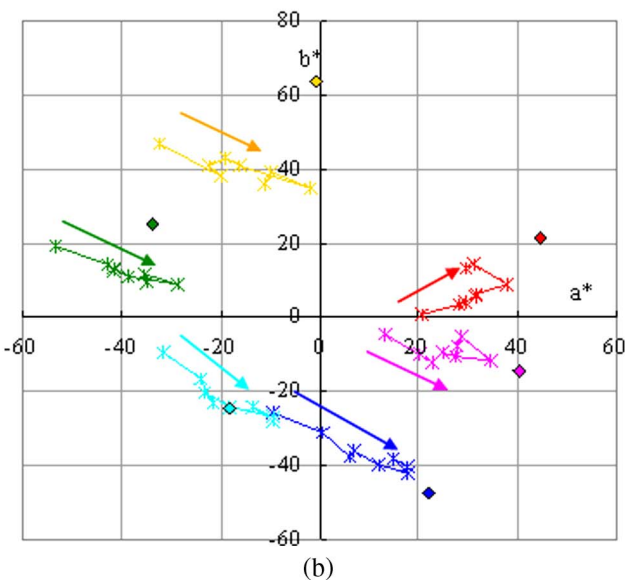
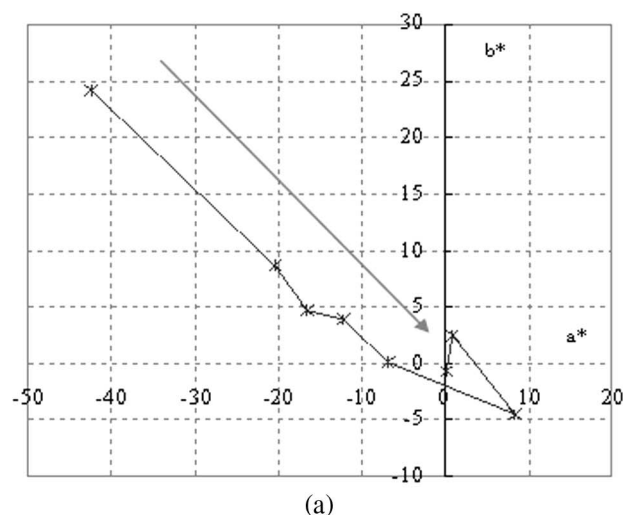


Fig. 9. (Color online) Color change depending on the incident angle of illumination beam (24 to  $38^\circ$ ). (a) White patch (No. 19 of MCC chart shown in Fig. 6). (b) B, G, R, Y, M, C color patches (Nos. 13 through 18 of MCC) are shown. The arrows indicate the direction of color shift with increasing incident angle of the illumination beam.

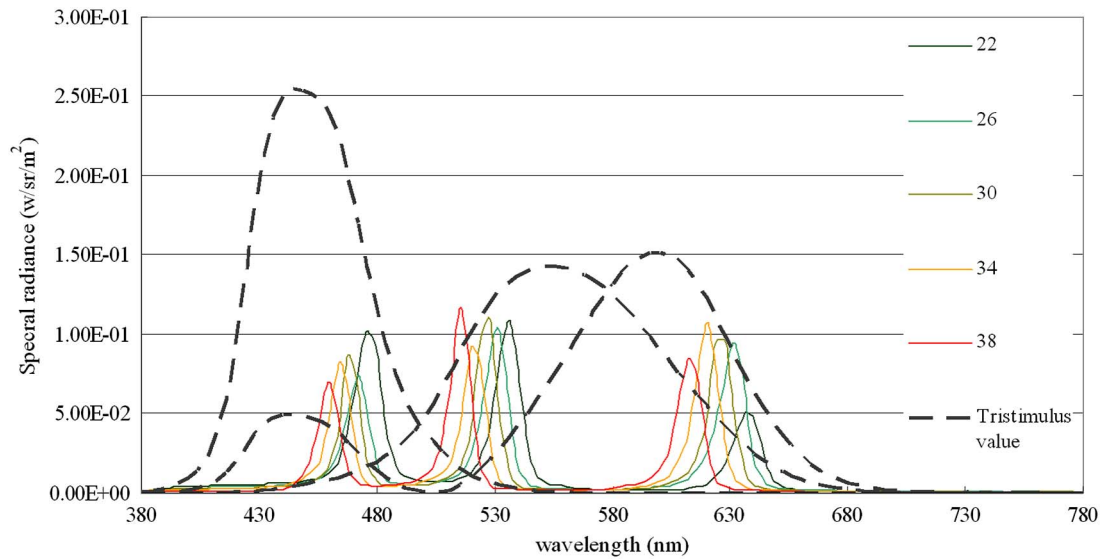


Fig. 10. (Color online) Reconstructed spectra of green patch (No. 14) hologram for illumination angles, as the legend shows, from 22 to 38°.

[image shown in Fig. 6(b)], and the CIELAB color difference  $\Delta E$  is calculated using the following formula:

$$L^* = 116f(Y/Y_n) - 16$$

$$a^* = 500[f(X/X_n) - f(Y/Y_n)]$$

$$b^* = 200[f(Y/Y_n) - (Z/Z_n)]$$

$$f(\omega) = (\omega)^{1/3} \quad \omega > 0.008856$$

$$f(\omega) = 7.787(\omega) + 16/116 \quad \omega < 0.008856$$

$$\Delta E_{L^*a^*b^*} = \sqrt{(L_1^* - L_2^*)^2 + (a_1^* - a_2^*)^2 + (b_1^* - b_2^*)^2}. \quad (10)$$

The color differences between the original and holographic color patches are shown in Fig. 6(c). The average color difference is 17.0, which is not very small but can be roughly acceptable for some applications. Figure 7 also shows the color differences in the  $a^*b^*$  plane. With the incident illumination angle of 38 deg, the reconstructed colors are shifted from the original colors in the direction of reducing chroma. The reason for this type of color shift is considered to be the influence of background light.

Figure 8 shows the reproduced spectra selected from 24 color patches of the MCC chart. Looking at the detail of the spectral curves, it is found that the peak wavelength slightly varies. The spectral shift may be due to the spatial nonuniformity introduced by insufficient control of the chemical development process. This is one of the reasons for the color error.

Another reason for the error appearing in Fig. 6 is the noise appearing in the reconstructed image shown in Fig. 6(a). The noise originated from the speckle generated by the weak diffuser shown in Fig. 1. The use of a digital diffuser, which can reduce

this kind of speckle noise [18], is recommended for better image quality.

#### B. Analysis of Reproduced Colors by Different Illumination Angle

The color reproduced by HS depends on the illumination angle. Figure 9 shows the color shift of white and color [blue, green, red, yellow, magenta, and cyan (BGRYMC)] patches in MCC. In Fig. 9(a), the color change of the white patch for illumination angles 24 to 38 deg is shown. According to Bragg's law, the wavelength of reconstructed light becomes shorter when the incident illumination beam angle increases. However, the colors do not necessarily move to bluish even though the reconstructed wavelengths of the primary light become shorter, as shown in Fig. 9. This is because of the peak wavelength of the reconstructed light of HS.

As shown in Fig. 10, any peak wavelength of the red primary is longer than the peak wavelength of

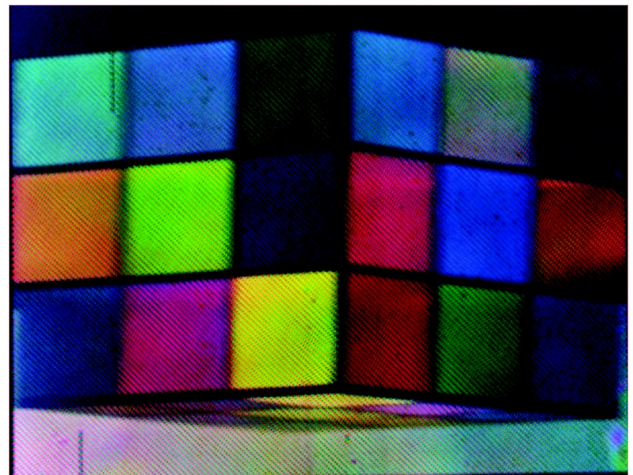


Fig. 11. Reconstruction of cubic 3D hologram image where the proposed color management technique was applied.

the color-matching function of  $X$ , that of green is shorter than  $Y$ , and that of blue is longer than  $Z$ . As a result, when the peak wavelength becomes shorter,  $X$  and  $Z$  increase and  $Y$  decreases. According to the relationship between  $XYZ$  and  $L^*a^*b^*$  described by Eq. (10), we can say that the colors shift in the direction of larger  $a^*$  and smaller  $b^*$ .

### C. 3D Image Reconstruction

Finally, a hologram of a 3D object is printed by introducing the color management described above. The reconstruction image of a hologram of a 3D cube is shown in Fig. 11. The color patches of the MCC chart are attached on the surfaces of the cube in Fig. 11. By introducing the color management, the colors of the cube can be reproduced naturally.

## 6. Conclusion and Future Work

In this article, we demonstrate the method and the preliminary experimental results of color management in a holoprinter. The color difference is not very small, but roughly the specified color can be obtained. We also discuss the color shifts with the variation of illumination beam angle and show that roughly the specified colors are still reproduced within a certain range of incident angle variation. The color difference can be minimized if the evaluation system is more accurate.

The following list gives the issues for future investigation in color management of holoprinters, and the result will be reported later.

1. The background light in the reconstruction of HS is large, and the influence from the background affects the color reproducibility. Even though the background light is included in the model, the color gamut reduces in dark colors, and color control becomes difficult. The main reason of background light is the scattering noise on the hologram plane. The exposed holographic material becomes white due to light scattering. It is expected to be decreased by using a photopolymer material, in which the scattering is much smaller.

2. The overlaps of adjacent elementary holograms are observed in the experiment but have not been verified. The cross talk between elementary holograms may cause channel dependency because elements of different primary colors influence each other. The effect of overlapped exposure should be addressed in future.

3. Pixel dependencies within an image for an elementary hologram, which are explained in Sec. 3.D, is one of the difficult problems because the pixel-based color conversion is insufficient if such pixel dependency is significant. If needed, a method to compensate for the pixel dependency should be developed for high-quality color management.

4. The noise and other causes of spatial inhomogeneity should be also addressed. The main reason of noise observed in the reconstructed image is the weak diffuser shown in Fig. 1 as explained in

Subsection. 4.D. It can be improved by replacing the weak diffuser with a digital diffuser designed for low speckle noise. Another source of spatial inhomogeneity is the nonuniformity originating from the chemical development and bleaching process. The chemical process also affects the diffraction efficiency and thickness variation of the recording material. By using photopolymer material, such instability is expected to be improved.

This digital color management technology will support the applications of holographic 3D display in the future, and the method presented in this article would avail the improvement of color quality of HS printed from digital 3D data.

The authors acknowledge Toppan Printing Co., Ltd. for the support on the development of the holoprinter system.

## References

1. M. Yamaguchi, N. Ohyama, and T. Honda, "Holographic three-dimensional printer: new method," *Appl. Opt.* **31**, 217–222 (1992).
2. M. A. Klug, M. W. Halle, and P. M. Hubel, "Full color ultragrams," *Proc. SPIE* **1667**, 110–119 (1992).
3. M. A. Klug, A. Klein, W. Plesniak, A. Kropp, and B. Chen, "Optics for full-parallax holographic stereograms," *Proc. SPIE* **3011**, 78–88 (1997).
4. A. Shirakura, N. Kihara, and S. Baba, "Instant holographic portrait printing system," *Proc. SPIE* **3293**, 246–253 (1998).
5. E. van Nuland, W. C. Spierings, and N. Govers, "Development of an office holoprinter V," *Proc. SPIE* **2652**, 62–69 (1996).
6. S. Zacharovas, "Advances in digital holography," in *Proceedings of the International Workshop on Holographic Memories & Display* (IWHM, 2008), pp. 55–67.
7. S. Frey, A. Thelen, S. Hirsch, and P. Hering, "Generation of digital textured surface models from hologram recordings," *Appl. Opt.* **46**, 1986–1993 (2007).
8. M. Takano, H. Shigeta, T. Nishihara, M. Yamaguchi, S. Takahashi, N. Ohyama, A. Kobayashi, and F. Iwata, "Full-color holographic 3D printer," *Proc. SPIE* **5005**, 126–136 (2003).
9. S. Maruyama, Y. Ono, and M. Yamaguchi, "High-density recording of full-color full-parallax holographic stereogram," *Proc. SPIE* **6912**, 12–22 (2008).
10. H. Bjelkhagen and E. Mirlis, "Color holography to produce highly realistic three-dimensional images," *Appl. Opt.* **47**, A123–A133 (2008).
11. R. S. Berns, "Methods for characterizing CRT display," *Displays* **16**, 173–182 (1996).
12. L. Jiménez del Barco, J. A. Díaz, J. R. Jiménez, and M. Rubiño, "Considerations on the calibration of color displays assuming constant channel chromaticity," *Color Res. Appl.* **20**, 377–387 (1995).
13. S. J. Zacharovas, A. M. Rodin, D. B. Ratcliffe, and F. R. Vergnes, "Holographic materials available from Geola," *Proc. SPIE* **4296**, 206–212 (2001).
14. L. DeMarsh, "Colorimetry for HDTV," *IEEE Trans. Consumer Electron.* **37**, 1–6 (1991).
15. D. H. Brainard, D. G. Pelli, and T. Robson, "Display characterization," in *Encyclopedia of Imaging Science and Technology* (Wiley, 2002), pp. 172–188.
16. D. H. Brainard, "Calibration of a computer controlled color monitor," *Color Res. Appl.* **14**, 23–34 (1989).
17. N. Ohta, *Color Engineering* (Academic, 2008).
18. M. Yamaguchi, H. Endoh, T. Honda, and N. Ohyama, "High-quality recording of a full-parallax holographic stereogram with a digital diffuser," *Opt. Lett.* **19**, 135–137 (1994).